A Cloud-Based Flexibility Estimation Method for Domestic Heat Pumps

C. Baumann[1], G. Huber[1], M. Preißinger[1], and P. Kepplinger[1*]

[1]Josef Ressel Centre for Intelligent Thermal Energy Systems,
illwerke vkw Endowed Professorship for Energy Efficiency, Research Center Energy,
Vorarlberg University of Applied Sciences, Hochschulstrasse 1, 6850 Dornbirn, Austria

*Corresponding author: peter.kepplinger@fhv.at

Abstract

Flexibility estimation is the first step necessary to incorporate building energy systems into demand side management programs. We extend a known method for temporal flexibility estimation from literature to a real-world residential heat pump system, solely based on historical cloud data. The method proposed relies on robust simplifications and estimates employing process knowledge, energy balances and manufacturer's information. Resulting forced and delayed temporal flexibility, covering both domestic hot water and space heating demands as constraints, allows to derive a flexibility range for the heat pump system. The resulting temporal flexibility lay within the range of 24 minutes and 6 hours for forced and delayed flexibility, respectively. This range provides new insights into the system's behaviour and is the basis for estimating power and energy flexibility - the first step necessary to incorporate building energy systems into demand side management programs.

Keywords: flexibility estimation, heat pump, intelligent thermal energy systems.

Introduction

Flexibility estimation of building energy systems (BES) provides the basis for residential demand side management (DSM), which manages consumption to improve overall system efficiency [1]. Chen et al. [1] classify and discuss reliable methods for DSM with thermal energy storages (TES) to provide flexibility in buildings, concluding division of flexibility into positive and negative components as essential.

A typical configuration of BES for DSM studied in literature comprise heat pump (HP) systems for space heating (SH) [2] or domestic hot water (DHW) supply [3], which exhibit flexibility via building mass and thermal energy storage [4, 5]. Arteconi et al. [2] analyzed HPs with radiators, underfloor heating and TES, depicting influences on the building occupant's thermal comfort. Underfloor heating (high thermal inertia) maintained the thermal comfort even without TES, whereas radiators (low thermal inertia) made the inclusion of a TES necessary. Kepplinger et al. [3] investigated a cost-optimization-driven domestic hot water heater (DHWH) by taking user thermal comfort and reduced sensor information for state estimation into account [6]. Results showed energy and cost savings compared to alternatively night-tariff switched DHWHs [3]. D'hulst et al. [4] showed that DHWH with TES show the highest potential of all household appliances for DSM to provide the most stable flexibility over time. Hewitt et al. [5] stated, that the role of HPs cannot be underestimated in an effort to integrate greater amounts of electricity since the dynamics of even relatively simple buildings already allows a degree of thermal management.

However, to benefit from the potentials reported, flexibility estimation has to be provided at low technological and economic costs [7]. Finding an optimal integration solution with the lowest cost, potential flexibility should already be considered in planning phase of the HP system; for scalable solutions and broader knowledge about flexibility use, HP pools should be considered

[7, 8]. Different flexibility estimation and assessment methods are discussed in literature [4, 8, 9, 10, 11, 12], but rarely applied to settings of real-world implementation, struggling with reduced sensor information [6]. Several studies in literature quantify flexibility, but a unique definition still does not exist; but it is clear that the inclusion of DSM becomes increasingly important [9, 8]. Arteconi et al. [8] also illustrate that flexibility is mostly characterized by: amount of power change, duration of change, rate of change, response time, shifted load, and maximal hours of load shifted. Additionally, they assess the potential during operation time with the occurrence of specific events like demand response control signals, where the most relevant parameters are temporal flexibility, power capacity, and energy shifted.

Similar to Arteconi et al. [8], Fischer et al. [10] introduce characteristic flexibility parameters like maximum power, mean power, shiftable energy, duration time, and regeneration time for a heat pump pool, suggesting duration of activation and regeneration as new flexibility parameters to get insights on shifting cycles. Nuytten et al. [11] separate flexibility estimation into a forced and delayed component, where depending on BES including TES, has an almost linear influence on flexibility. Thereby, no distinction between SH and DHW was made. Stinner et al. [12] distinguish between temporal, power and energy flexibility including average and cycle flexibilities, which makes aggregating flexibilities on a higher level possible, e.g. district level or electrical grid. In summary, the literature shows a gap, where the distinction of flexibility between DHW and SH operation is neglected and real-world implementation, struggling with reduced sensor information is rarely considered. We adapt the method proposed by Stinner et al. [12] to estimate the temporal flexibility of a real-world heat pump system supplying SH and DHW based on historical cloud data available to a heat pump manufacturer and operator.

Methodology

According to Stinner et al. [12], temporal flexibility can be divided into forced and delayed temporal flexibility. The former refers to the maximum operation time of the HP until the storage is fully charged, the latter to the time until full depletion of the storage. We adapt this method to derive a combined forced and delayed flexibility range (Figure 1, bottom). A real-world heat pump system with stratified storage for DHW and SH is considered (Figure 1, top). Due to usual cost reductive measures, the system comes without all needed pressure, temperature, power and flow metering. Instead, our approach only uses a given compressor's map of characteristics and those sensors which are needed for operation. Measurements available include evaporation temperature, flow temperature, DHW temperature, SH temperature, and operation times. These reduced information forces us to make assumptions on the calculation of electrical power P_{el}, cooling power $\dot{Q}_{\text{cool}}$, DHW demand $\dot{Q}_{\text{DHW}}$ and SH demand $\dot{Q}_{\text{SH}}$ (Figure 1, middle). On the one hand, determining electrical power and cooling power by using the compressor's map of characteristics, on the other hand determining DHW and SH demand by using process knowledge and forward calculation. The proposed method not only can be transferred to other heat pump systems but also provides the basis for a cloud-based system to estimate the flexibility of a fleet of heat pumps. In the following sections, the necessary steps are explained in more detail.

Defining operation times for DHW and SH via compressor run time sensors allows distinguishing the specific operation mode. The heat pump either is operated to supply heat for DHW or SH, also it might be switched off, i.e., the total set of discrete-time steps $\mathcal{T} = \{t_1, \cdots, t_n\}$ can be divided into disjoint subsets,

$$\mathcal{T} = \mathcal{T}_{\text{DHW}} \sqcup \mathcal{T}_{\text{SH}} \sqcup \mathcal{T}_{\text{OFF}}. \tag{1}$$

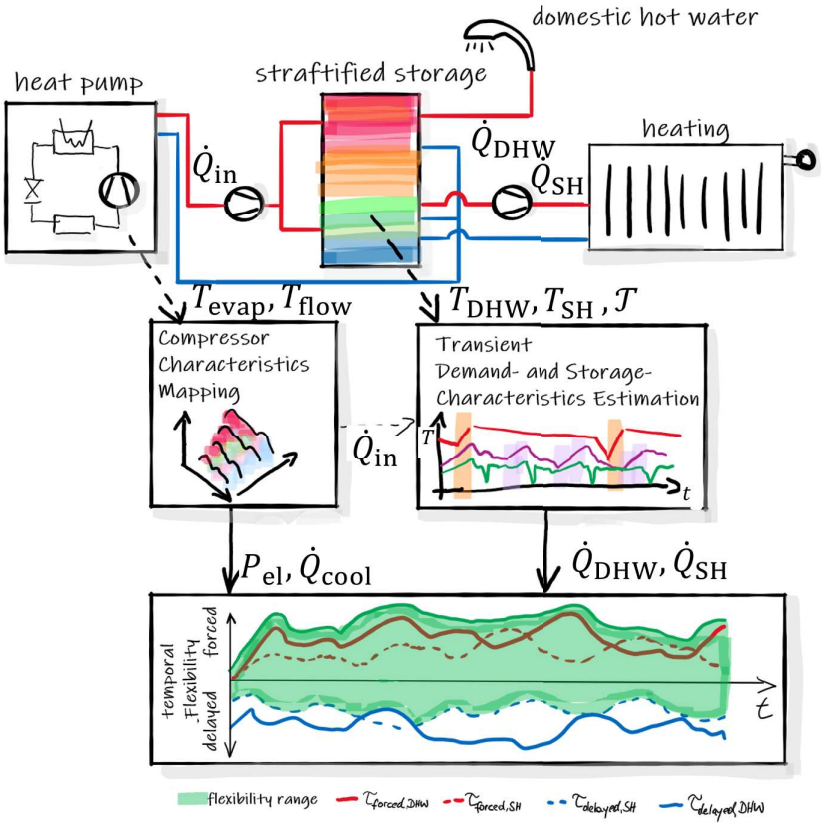

Figure 1. Schematic of the method proposed to derive a temporal flexibility estimation.

To easily formulate relationships for both operation modes, we refer to the subscript $\cdot_{\text{MODE}}$, e.g., $\mathcal{T}_{\text{MODE}}$ can refer to $\mathcal{T}_{\text{SH}}$ or $\mathcal{T}_{\text{DHW}}$.

Polynomial approximation of the compressor's map of characteristics is used to calculate the cooling power $\dot{Q}_{\text{cool}}$ and electrical power P_{el} of the compressor, as no power or energy meter is available. The required power is estimated by using the foregoing estimated operation times $\mathcal{T}$ for MODE and polynomials are given by the manufacturer. The power polynomials require condensation temperature T_{cond} and evaporation temperature T_{evap} for the estimation. Since the condensation temperature is not recorded by measurement, the flow temperature is used as an estimate of the condensation temperature, i.e. $T_{\text{cond}} \approx T_{\text{flow}}$. the coefficients $C_0 - C_9$ of the polynomials to estimate electric power and cooling power are provided by the manufacturer,

$$\begin{aligned} P_{\text{el,MODE}} &= C_0 + C_1 T_{\text{evap}} + C_2 T_{\text{flow}} + C_3 T_{\text{evap}}^2 + C_4 T_{\text{evap}} T_{\text{flow}} + C_5 T_{\text{flow}}^2 \\ &\quad + C_6 T_{\text{evap}}^3 + C_7 T_{\text{flow}} T_{\text{evap}}^2 + C_8 T_{\text{evap}} T_{\text{flow}}^2 + C_9 T_{\text{flow}}^3, \end{aligned} \tag{2}$$

$$\begin{aligned} \dot{Q}_{\text{cool,MODE}} &= C_0 + C_1 T_{\text{evap}} + C_2 T_{\text{flow}} + C_3 T_{\text{evap}}^2 + C_4 T_{\text{evap}} T_{\text{flow}} + C_5 T_{\text{flow}}^2 \\ &\quad + C_6 T_{\text{evap}}^3 + C_7 T_{\text{flow}} T_{\text{evap}}^2 + C_8 T_{\text{evap}} T_{\text{flow}}^2 + C_9 T_{\text{flow}}^3. \end{aligned} \tag{3}$$

Then, at each timestep t, the heating power $\dot{Q}_{\text{in}}$ for both modes of operation, DHW and SH, can be calculated as follows:

$$\dot{Q}_{\text{in,MODE}}(t) = P_{\text{el,MODE}}(t) + \dot{Q}_{\text{cool,MODE}}(t). \tag{4}$$

Determination of heat transfer characteristics $(UA)_{\text{DHW}}$ and $(UA)_{\text{SH}}$ of the TES, as well as the thermal storage capacities C_{DHW} and C_{SH} are based on the hydraulic scheme provided by the manufacturer. Assuming a perfectly stratified storage enabled through stratification switches leads to the following energy balances for each operation mode:

$$\frac{C_{\text{MODE}}dT}{dt} = \dot{Q}_{\text{in,MODE}}(t) - \dot{Q}_{\text{loss,MODE}}(t) - \dot{Q}_{\text{dem,MODE}}(t). \tag{5}$$

We assume the heat transfer from the heat pump to the storage to take place in the specific storage layer and no overlapping of the two storage layers at all times.

TES capacities C_{DHW} and C_{SH} are determined, identifying the shortest heating period, for which losses are assumed to be negligible and no demand occurs:

$$C_{\text{MODE}} = \frac{\sum_{t_1}^{t_2} \dot{Q}_{\text{in,MODE}}(t)\Delta t}{T_{\text{MODE}}(t_2) - T_{\text{MODE}}(t_1)}, \text{ where} \tag{6}$$

$$(t_1, t_2) = \arg \min_{t_1, t_2 \in \mathcal{T}_{\text{MODE}}} t_2 - t_1, \text{ such that} \tag{7}$$

$$T_{\text{MODE}}(t_2) = T_{\text{up,MODE}}, \tag{8}$$

$$T_{\text{MODE}}(t_1) = T_{\text{low,MODE}}, \tag{9}$$

$$\dot{Q}_{\text{in,MODE}}(t) > 0 \; \forall t \in [t_1, t_2]\,. \tag{10}$$

Here ($T_{\text{up, MODE}}$ and $T_{\text{low, MODE}}$) refer to the upper and lower set point temperature, respectively.

Analogously in equation (15), heat transfer characteristics $(UA)_{\text{DHW}}$ and $(UA)_{\text{SH}}$ have been determined, by using maximum duration non-heating periods, assuming to reflect no demand,

$$(UA)_{\text{MODE}} = \frac{\sum_{t_1}^{t_2} \dot{Q}_{\text{loss,MODE}}(t)\Delta t}{T_{\text{MODE}}(t_2) - T_{\infty}}, \text{ where} \tag{11}$$

$$(t_1, t_2) = \arg \max_{t_1, t_2 \in \mathcal{T}_{\text{OFF}}} t_2 - t_1, \text{ such that} \tag{12}$$

$$T_{\text{MODE}}(t_1) = T_{\text{up,MODE}}, \tag{13}$$

$$T_{\text{MODE}}(t_2) = T_{\text{low,MODE}}, \tag{14}$$

$$\dot{Q}_{\text{in,MODE}}(t) = 0 \; \forall t \in [t_1, t_2]\,. \tag{15}$$

Reformulating equation (5) with parameters $(UA)_{\text{MODE}}$ and C_{MODE} allows determining the demand as follows:

$$\begin{aligned}\dot{Q}_{\text{dem,MODE}}(t) = \dot{Q}_{\text{in,MODE}}(t) - (UA)_{\text{MODE}}\big(T_{\text{MODE}}(t) - T_{\infty}(t)\big) \\ - C_{\text{MODE}}\big(T_{\text{MODE}}(t+\Delta t) - T_{\text{MODE}}(t)\big), \forall t \in \mathcal{T}_{\text{MODE}}.\end{aligned} \tag{16}$$

The maximum available TES capacity is determined as:

$$E_{\text{max,MODE}} = C_{\text{MODE}}\Delta T_{\text{MODE}} = C_{\text{MODE}}(T_{\text{up, MODE}} - T_{\text{low, MODE}}). \tag{17}$$

To estimate the maximum heating power for the present mode of operation, the highest value in data is chosen:

$$Q_{\text{max,MODE}} = \max_{t \in \mathcal{T}_{\text{MODE}}} \dot{Q}_{\text{in,MODE}}(t)\Delta t. \tag{18}$$

Stinner et al. [12] define the forced temporal flexibility as the period for each time step where the power surplus of the heat pump working at maximum power, will be enabled to fully charge the in-situ located TES from a fully discharged state. To this end, heating demand, heat loss and generated heat (Figure 2, left). Hence, repeating this process for every time step t with an assumed discharged TES at the beginning, the forced temporal flexibility $\tau_{\text{forced,MODE}}(t_0)$ can be determined by solving:

$$\sum_{t=t_0}^{\tau_{\text{forced,MODE}}(t_0)} Q_{\text{max,MODE}} - Q_{\text{dem, MODE}}(t) - Q_{\text{loss, MODE}}(t) \overset{!}{\geq} E_{\text{max, MODE}}. \tag{19}$$

In the same way, the delayed temporal flexibility is defined as the period the heat pump can be switched off until the full energetic depletion of the TES is reached from a fully charged state. Heat demand and heat losses lead to the depletion of the TES (Figure 2, right). Repeating this process for every time step t, the delayed temporal flexibility $\tau_{\text{delayed,MODE}}(t_0)$ can be determined by solving:

$$\sum_{t=t_0}^{\tau_{\text{delayed,MODE}}(t_0)} Q_{\text{dem, MODE}}(t) + Q_{\text{loss, MODE}}(t) \overset{!}{\geq} E_{\text{max, MODE}} \tag{20}$$

Comparing the heat generated $Q_{\text{in,MODE}}$ and the heat demand $Q_{\text{dem, MODE}}$ including storage losses $Q_{\text{loss, MODE}}$, allows to calculate the forced and delayed temporal flexibility for each time step, resulting in a function $\tau_{\text{forced}}(t)$ and $\tau_{\text{delayed}}(t)$, respectively.The feasible operation has to take into account both constraining demands, resulting in the combined flexibility range (Figure 1, bottom). Since generated heat input is operation mode dependent, both thermal capacities are exploited. Hence, both forced flexibilities accumulate to a combined forced temporal flexibility where the function describes the upper bound of the flexibility range. Opposing, delayed temporal flexibility as lower bound of the flexibility range takes the minimum available time of both DHW and SH into account. Assuming the decision for full energetic depletion of the chosen storage capacity, only one limit can be exploited at a time, otherwise comfort and system boundaries will be violated.

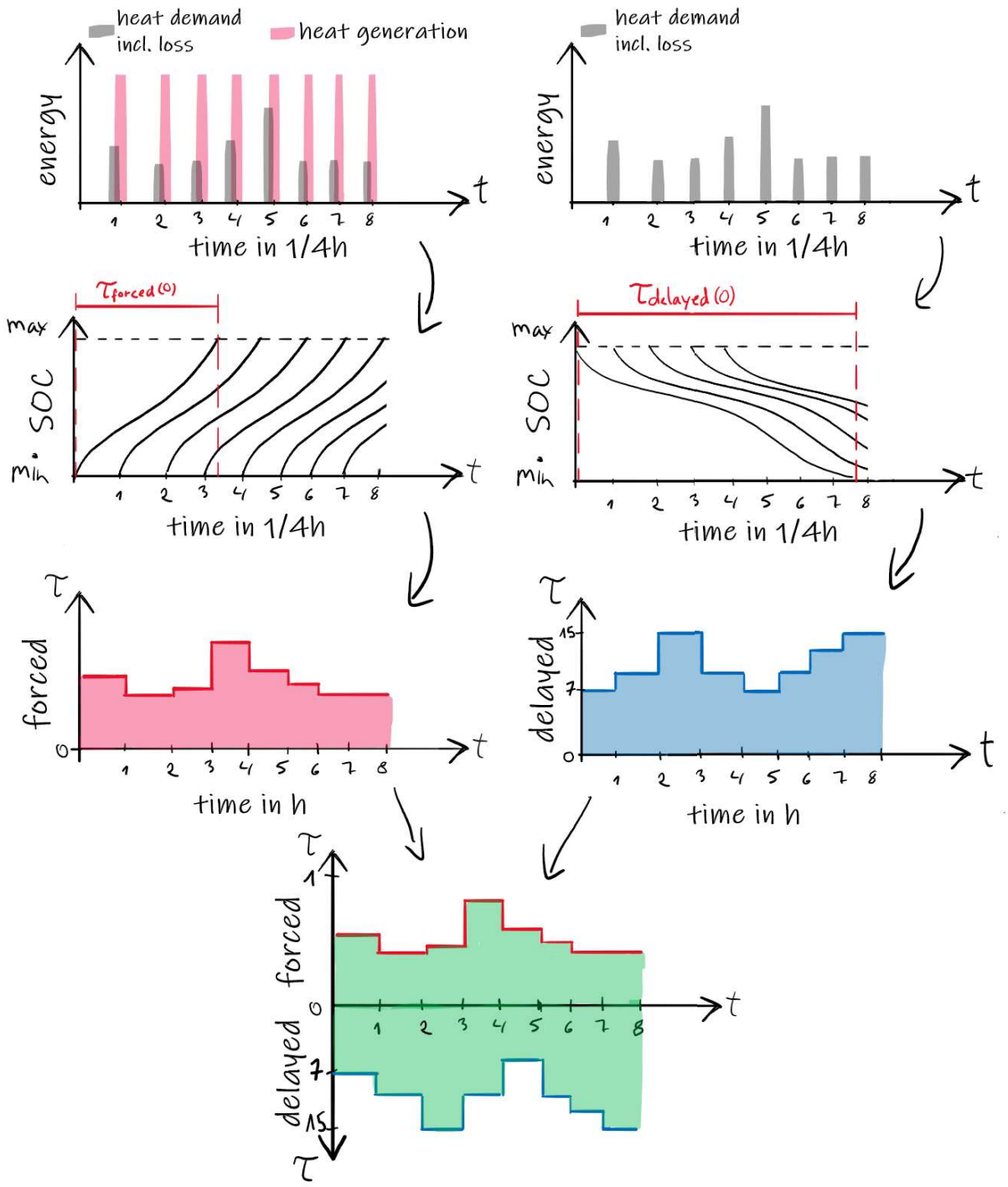

Figure 2. Schematic of the estimation methodology for forced (left) and delayed (right) temporal flexibility, according to Stinner et al. [12].

Example & Results

Applying the methodology to a real-world heat pump system, the specifics of the system, including the hydraulic scheme and sensor positions, have to be taken into account. We investigate a Weider Weitrona SW151 brine/water heat pump including a stratified storage with a capacity of 1000 litres for DHW and SH, based in Vorarlberg, Austria, showing significant seasonal variation. (Figure 1, top).

Assuming a perfect stratification through stratification switches leads to the determination of the thermal capacity of 2.3 kWh for DHW and 4.6 kWh for SH, respectively. Analogously, the heat transfer characteristic $(UA)_{\mathrm{MODE}}$ could be determined with 0.7 W/K for DHW and 0.9 W/K for SH, respectively.

Based on that, iterative calculation of heat demand and heat loss for DHW and SH is implemented and lead to the necessary profiles. Eventually, the determination of maximum thermal storage capacity and maximum possible heating power provides the basis for the forced and delayed temporal flexibility estimation. The temporal flexibility estimation is based on a data set of one year.

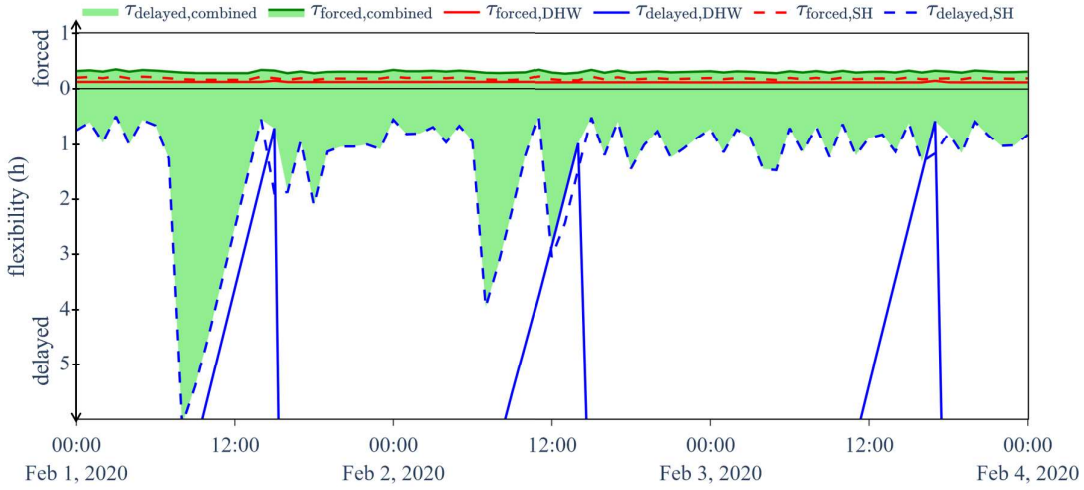

Figure 3. Determined forced and delayed temporal flexibility for DHW-, SH- and the combined mode. Forced temporal flexibility (red) and delayed temporal flexibility (blue) shown for DHW/SH mode (solid/dashed). Combined temporal flexibility range (green area) derived by boundary conditions of forced and delayed temporal flexibility of DHW and SH.

Determined forced and delayed flexibility for DHW and SH are depicted for three consecutive days in winter (Figure 3). Combined forced flexibility is derived by an accumulation of forced flexibility for DHW and SH, shown as green curve. Thus, a maximum combined forced flexibility of 24 minutes can be determined. The possible forced flexibility range lay within 0 and 24 minutes. Analogously, finding the minimum available delayed flexibility of DHW and SH leads to the opposing maximum available delayed flexibility of the combined system. In the time series of the three consecutive days, a maximum delayed flexibility of 6 hours can be determined. The possible delayed flexibility range lays within 0 and 6 hours. Derived from these two ranges, the overall range lay within 24 minutes forced and 6 hours of delayed flexibility.

While Figure 3 is taking different operation modes into account and shows the combined result, Figure 4 takes the whole year calculation of combined forced and delayed flexibility into account, comparing three consecutive days of winter, summer and transition season. For forced flexibility, peak times during the winter season, followed by intermediate flexibilities of transition and summer period, are observed. Hence, the lowest forced flexibilities are available during summer, where the demand for SH is lowest. Opposing, delayed flexibility is highest during the transition season. The decreased potential is identified in winter, continued by the summer season. Contrary to peak flexibility, the highest delayed base flexibility is identified

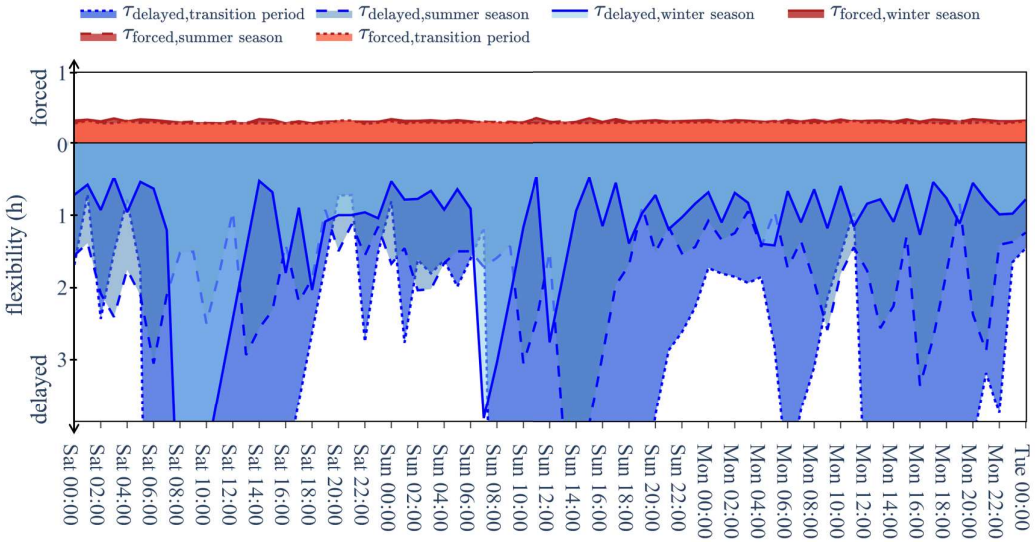

Figure 4. Comparison of the temporal flexibility range of three consecutive days during winter (solid), summer (dashed) and in the transition period (dotted) marked as forced (red) and delayed flexibilities (blue).

during summer season, followed by the transition and winter period. Comparing the amount of possible flexibility in the example investigated, delayed flexibility shows a tremendously higher potential than the forced operation.

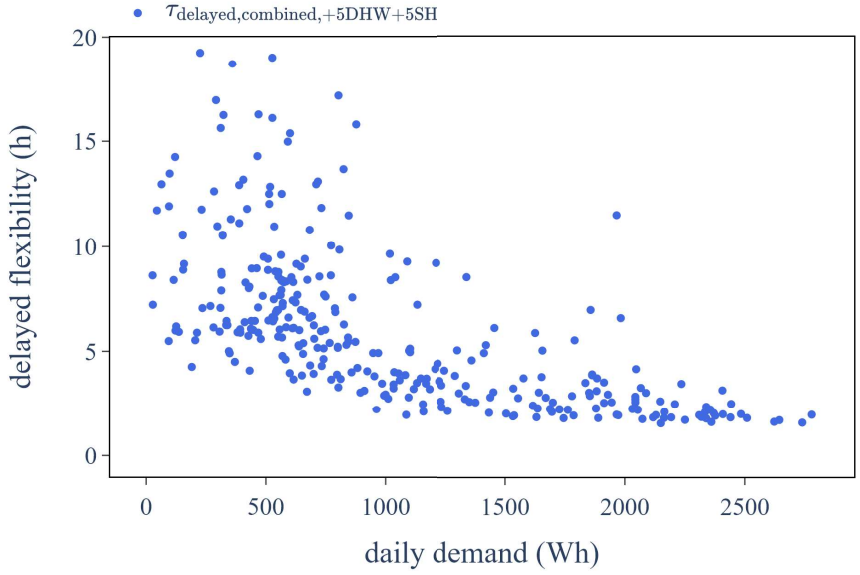

Figure 5. The daily mean of delayed temporal flexibility plotted against daily sum of DHW & SH demand over a one year period.

Considering possible forced and delayed flexibility in more detail, four different scenarios for DHW and SH temperature spreads (+5K) are investigated: reference case, +5DHW, +5SH and +5DHW+5SH. Since forced and delayed flexibility show contrary flexibility characteristics due

to heat demand, the relation between the daily mean of flexibility and the daily sum of DHW and SH demand over a one year period is investigated. A decrease in the available delayed flexibility correlates with rising demand (Figure 5). Consequently, the highest flexibilities are found for days only showing little tap events within the range from 200 to 800 Wh.

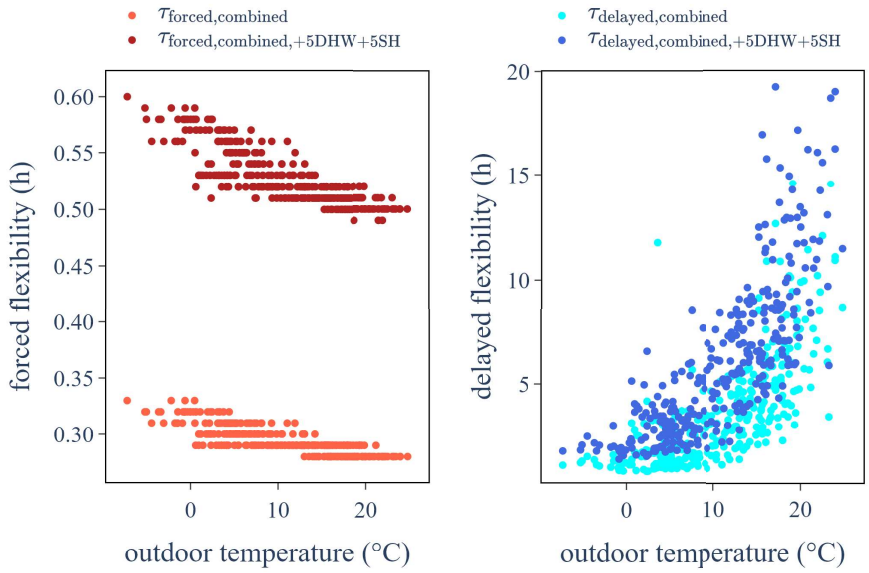

Figure 6. Left: The daily mean of combined forced temporal flexibility plotted against the daily mean of outdoor temperature over a one year period. Right: The daily mean of delayed temporal flexibility plotted against the daily mean of outdoor temperature over a one year period.

Figure 6 left refers to the forced flexibility, showing two of the scenarios investigated. The daily mean of forced flexibility is plotted against the daily mean of outdoor temperature over a one year period. A decrease in the available forced flexibility with rising outdoor temperatures independently from the scenarios is shown. Taking the same decay in every scenario into account, a linear offset factor can be observed: 1.2 for +5DHW, 1.6 for +5SH and 1.8 for +5DHW+5SH (Figure 7, left). Hence, the increase of the combined temperature spread +5DHW+5SH leads to the highest potential. Comparison of the +5DHW and the +5SH scenario shows a higher flexibility per Kelvin in the SH scenario, which is derived by higher thermal capacity.

In contrast to forced flexibility, an increase in the available flexibility with rising outdoor temperatures can be observed (Figure 6, right). For delayed flexibility, low SH use is related to higher outdoor temperatures and provides more available capacity. The highest flexibility of the investigated scenarios is observed in the combined +5DHW+5SH scenario. Taking the same increase in every scenario into account, an exponential offset factor can be observed: 1.1 for +5DHW, 1.6 for +5SH and 1.7 for +5DHW+5SH (Figure 7, right).

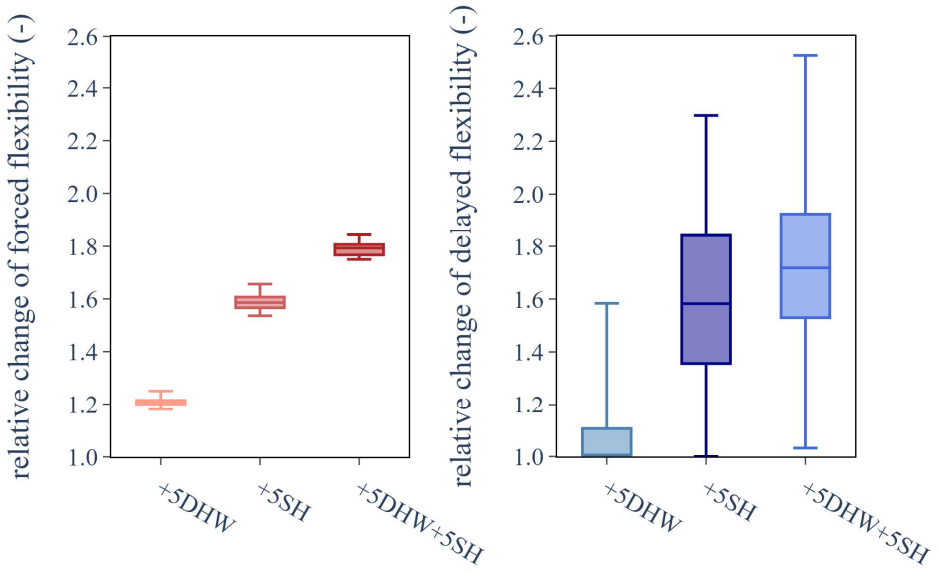

Figure 7. Box-plots of the relative change of forced (left) and delayed (right) temporal flexibility of different scenarios considered.

Discussion

Setup dependent thermal capacities and heat demand behaviour of DHW and SH decide on the flexibility characteristic of the system. In the real-world application, forced and delayed temporal flexibility showed quite different behaviour on demand. While forced flexibility rose with high demand, delayed flexibility showed a decrease. Since SH demand and thermal capacity dominated over the DHW case, forced and delayed temporal flexibility have been strongly dependent on seasonal variations. Depending on the sizing of thermal capacities in other system configurations, this may vary. Thus, an intelligent forecast of demand can lead to highly reliable flexibility forecast and use.

Delayed temporal flexibility showed a significantly higher potential in all cases and scenarios. Thus, in further application of flexibility range, an absolute difference of forced and delayed flexibility has to be considered.

Additionally, the calculation of the relative change of flexibility showed that minor increments of the limiting storage temperatures can lead to high improvements in forced and delayed flexibility. Exemplary for the +5SH scenario, an increment of 5 Kelvin led to an improvement of factor 1.6 in forced and delayed flexibility.

Conclusion

An extended method for flexibility estimation based on historical cloud data of a real-world heat pump system has been presented. The method proposed, relied on robust simplifications and estimates, employing process knowledge, energy balances and manufacturer's information. Resulting forced and delayed temporal flexibility, covering both, domestic hot water and space heating demands as constraints, allowed to derive a flexibility range for the heat pump system.

The simulation was conducted for an entire year. Forced and delayed temporal flexibility of each operation mode were calculated, deriving the combined flexibility, as well as the flexibility

range. In the reference case, the derived flexibility range lay within 24 minutes of forced and 6 hours of delayed temporal flexibility. The best-case scenario of three additionally investigated scenarios enhanced forced temporal flexibility by factor 1.8, delayed flexibility by about 1.7, respectively.

The proposed flexibility estimation method not only provides insights into the system's behaviour, it also enables the estimation of possible flexibility improvements and provides the basis for a cloud-based system to estimate the flexibility of a fleet of heat pumps. As temporal flexibility range is the basis for estimating power and energy flexibility, which is the first step necessary to incorporate building energy systems into demand side management programs, this work should be further extended.

Acknowledgement: The financial support by the Austrian Federal Ministry for Digital and Economic Affairs and the National Foundation for Research, Technology and Development and the Christian Doppler Research Association is gratefully acknowledged. The authors are grateful to the project partner Weider Wärmepumpen GmbH for the support and providing the real data.

References

[1] Yongbao Chen, Peng Xu, Jiefan Gu, Ferdinand Schmidt, and Weilin Li. Measures to improve energy demand flexibility in buildings for demand response (DR): A review. *Energy and Buildings*, 177:125–139, 2018.

[2] A. Arteconi, N.J. Hewitt, and F. Polonara. Domestic demand-side management (DSM): Role of heat pumps and thermal energy storage (TES) systems. *Applied Thermal Engineering*, 51(1):155–165, 2013. 00141.

[3] Peter Kepplinger, Gerhard Huber, and Jörg Petrasch. Autonomous optimal control for demand side management with resistive domestic hot water heaters using linear optimization. *Energy and Buildings*, 100:50–55, 2015.

[4] R. D'hulst, W. Labeeuw, B. Beusen, S. Claessens, G. Deconinck, and K. Vanthournout. Demand response flexibility and flexibility potential of residential smart appliances: Experiences from large pilot test in belgium. *Applied Energy*, 155:79–90, 2015.

[5] Neil J Hewitt. Heat pumps and energy storage – the challenges of implementation. *Applied Energy*, 89(1):37–44, 2012.

[6] Peter Kepplinger, Gerhard Huber, Markus Preißinger, and Jörg Petrasch. State estimation of resistive domestic hot water heaters in arbitrary operation modes for demand side management. *Thermal Science and Engineering Progress*, 9:94–109, 2019.

[7] David Fischer and Hatef Madani. On heat pumps in smart grids: A review. *Renewable and Sustainable Energy Reviews*, 70:342–357, 2017. 00005.

[8] Alessia Arteconi and Fabio Polonara. Assessing the demand side management potential and the energy flexibility of heat pumps in buildings. *Energies*, 11(7), 2018.

[9] John Clauß. Control strategies for building energy systems to unlock demand side flexibility – a review. *IBPSA Building Simulation 2017, San Francisco, 7-9 August 2017*, 2017.

[10] David Fischer, Tobias Wolf, Jeannette Wapler, Raphael Hollinger, and Hatef Madani. Model-based flexibility assessment of a residential heat pump pool. *Energy*, 118:853–864, 2017.

[11] Thomas Nuytten, Bert Claessens, Kristof Paredis, Johan Van Bael, and Daan Six. Flexibility of a combined heat and power system with thermal energy storage for district heating. *Applied Energy*, 104:583–591, 2013.

[12] Sebastian Stinner, Kristian Huchtemann, and Dirk Müller. Quantifying the operational flexibility of building energy systems with thermal energy storages. *Applied Energy*, 181:140–154, 2016.